

## Accelerating evaporative cooling of atoms into Bose-Einstein condensation in optical traps

Chen-Lung Hung, Xibo Zhang, Nathan Gemelke, and Cheng Chin

*James Frank Institute and Physics Department, The University of Chicago, Chicago, Illinois 60637, USA*

(Received 4 April 2008; published 24 July 2008)

We demonstrate a simple scheme to achieve fast, accelerating (runaway) evaporative cooling of optically trapped atoms by tilting the optical potential with a magnetic field gradient. Runaway evaporation is possible in this trap geometry due to the weak dependence of vibration frequencies on trap depth, which preserves atomic density during the evaporation process. Using this scheme, we show that Bose-Einstein condensation with  $\sim 10^5$  cesium atoms can be realized in 2–4 s of forced evaporation. The evaporation speed and energetics are consistent with the three-dimensional evaporation picture, despite the fact that atoms can only leave the trap in the direction of tilt.

DOI: [10.1103/PhysRevA.78.011604](https://doi.org/10.1103/PhysRevA.78.011604)

PACS number(s): 67.85.Hj, 05.30.Jp, 64.70.fm

The possibility to manipulate Bose-Einstein condensates (BECs) and degenerate Fermi gases of cold atoms in optical traps opens up a wide variety of exciting research; prominent examples include spinor condensates [1], Feshbach resonance in cold collisions [2], and BECs of molecules [3,4]. In many early experiments, condensates were first created in a magnetic trap and subsequently transferred to an optical dipole trap. These experiments could be greatly simplified after direct evaporation to BEC in optical traps as demonstrated in [5]. In this paper, we describe a further improvement on dipole-trap based evaporation, which allows for runaway cooling without significant increase in trap complexity.

Evaporative cooling proceeds by lowering the depth of a confining potential, which allows atoms with high kinetic energy to escape and the remaining particles to acquire a lower temperature and higher phase space density through rethermalization. Starting from a sample of precooled atoms in a dipole trap, one can perform forced evaporative cooling on optically trapped atoms by constantly reducing the trap depth until quantum degeneracy is reached. This method has been successful in creating rubidium BEC in a dipole trap [5], and has become a critical component in recent experiments on quantum gases of Cs [6], Li [7], K [8], and Yb [9]. In all of these experiments, forced evaporative cooling in the dipole trap is realized by reducing the intensity of the trapping beam, and consequently also the restoring forces. In a later discussion, we will refer to this approach as the trap-weakening scheme.

Evaporative cooling in optical traps remains one of the most time consuming and technically challenging steps in condensate production. Fundamentally, this is due to the fact that cooling by weakening the trapping potential inevitably reduces the collision rate. Here runaway (accelerating) evaporation is essentially impossible even with perfect evaporation efficiency and purely elastic collisions [10]. Within experimentally accessible times, the trap-weakening method puts a severe limit on the maximum gain in phase space density that one can reach. Several auxiliary schemes have been successfully implemented in order to increase the evaporation speed, including the dimple trap [6] and a zoom lens system [11]. These methods often increase the complexity of the apparatus or require delicate optical alignment or manipulation.

In this paper, we report a simple evaporative cooling

scheme which can be immediately implemented in many existing experiments. Instead of reducing the intensity of the trapping beam, we reduce the trap depth by applying an external force on the optically trapped atoms; see Fig. 1(a). This trap-tilting method entails only a weak reduction in confinement strength over a large range of potential depth and can significantly speed up the cooling process. Using this method, we demonstrate runaway evaporative cooling in a large volume dipole trap and reach Bose-Einstein condensation of cesium significantly faster than previous results [12]. Finally, we comment on the conditions for runaway evaporation in a tilted trap and investigate the dimensionality of atomic energy selection in the evaporation.

For this study, cesium atoms are first slowed by a Zeeman slower, collected in a magneto-optical trap (MOT) for 2 s, molasses precooled, and finally cooled and spin polarized by degenerate Raman-sideband cooling (dRSC) [13] to the lowest hyperfine ground state  $|F=3, m_F=3\rangle$ , where  $F$  is the total angular momentum and  $m_F$  is the magnetic quantum number; the apparatus for dRSC follows that in [13]. A crossed dipole trap and magnetic field gradient are employed to levitate and collect the cooled atoms. The dipole trap is formed by intersecting two laser beams on the horizontal ( $x$ - $y$ ) plane; both beams are extracted from a single-mode, single-frequency Yb fiber laser operating at the wavelength of 1064 nm, frequency offset by 80 MHz, focused to a  $1/e^2$  beam diameter of  $540\ \mu\text{m}$  ( $620\ \mu\text{m}$ ) and power of 1.9 W (1.6 W) in the  $y$  ( $x$ ) direction. In the absence of trap tilt, the trapping frequencies near the bottom of the potential well are  $(\omega_x^0, \omega_y^0, \omega_z^0) = 2\pi \times (17, 34, 38)$  Hz. During the dipole trap loading process, we switch on a uniform magnetic field of 58 G in the (vertical)  $z$  direction to improve the atom number following the loading process [6] and apply a levitating magnetic field gradient of  $B'_c = mg/\mu = 31.3$  G/cm, where  $mg$  is the gravitational force,  $\mu = 0.75\mu_B$  is the magnetic moment of the atoms in  $|3,3\rangle$ , and  $\mu_B$  is the Bohr magneton, see Fig. 1(b). After 1 s of thermalization and self-evaporation in the dipole trap, we ramp the magnetic field to 20.8 G, where three-body loss is minimized [14], and the field gradient to 37.8 G/cm in 1.85 s and begin our study on forced evaporation. At this point, which we define as time  $t=0$ , there are  $N_0 = 1.9 \times 10^6$  atoms in the trap with a temperature of  $T_0 = 470$  nK, peak atomic density of  $n = 3.8 \times 10^{12}$  cm $^{-3}$ , and peak collision rate

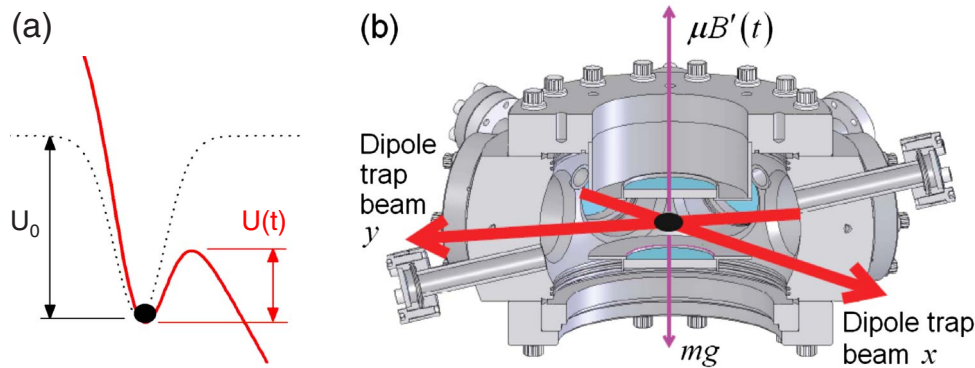


FIG. 1. (Color online) Trap-tilt based evaporation and experimental apparatus. (a) Trap depth  $U$  decreases when an external potential gradient is applied to the optically trapped atoms. (b) Apparatus for evaporation of cesium atoms (black dot) in a crossed-beam dipole trap. A strong, slowly varying magnetic field gradient  $B'(t)$  over-levitates the atoms with magnetic moment  $\mu$  against gravitational pull  $mg$  and evaporates them upward.

of  $\Gamma_0=133 \text{ s}^{-1}$ . The background collision rate is below  $0.02 \text{ s}^{-1}$ .

We perform forced evaporative cooling by linearly increasing the magnetic field gradient  $B'$  from 37.8 to 41.4 G/cm in 2.2 s and then to 43.5 G/cm in another 3 s, which reduces the calculated trap depth from  $3.0 \mu\text{K}$  to  $1.0 \mu\text{K}$  and then to  $170 \text{ nK}$ . The magnetic field and dipole trap intensity are kept constant throughout the process. To evaluate the cooling performance, we interrupt the evaporation at various times to measure the particle number  $N$ , temperature  $T$ , and trap frequencies  $\omega_{x,y,z}$ . Particle number and temperature are extracted from absorption images taken at low magnetic fields, following a 70 ms time-of-flight expansion at  $B=17 \text{ G}$  to minimize the collisions and  $B'=B'_c$  to levitate the atoms. Trap frequencies are measured from small amplitude oscillations of the atomic momentum by abruptly displacing the trap center. Peak phase space density is calculated from  $\phi=n\lambda_{dB}^3$ , where  $n=N\omega_x\omega_y\omega_z(m\lambda_{dB}/h)^3$  is the peak atomic density,  $\lambda_{dB}=h(2\pi mk_B T)^{-1/2}$  is the thermal de Broglie wavelength,  $k_B$  is the Boltzmann constant, and  $h$  is the Planck constant. Collision rates are calculated as  $\Gamma=n\langle\sigma v\rangle$ , where the elastic collision cross section is  $\sigma=8\pi a^2$ , scattering length at 20.8 G is  $a=200a_0$  [15], and  $\langle v\rangle=(16k_B T/\pi m)^{1/2}$  is the mean relative velocity.

After 4 s of forced evaporative cooling, we observe Bose-Einstein condensation from the appearance of bimodality and anisotropic expansion in time-of-flight images. At this point, the temperature is  $64 \text{ nK}$  and total particle number is  $5 \times 10^5$ . An almost pure condensate with  $10^5$  atoms was obtained after another 2.5 s. In this evaporation process, the mean truncation parameter is calculated to be  $\bar{\eta}=\langle U/k_B T\rangle=6.5(3)$ , and the evaporation efficiency is  $\bar{\gamma}_{ev}=-\ln(\phi/\phi_0)/\ln(N/N_0)=3.4$ . We observe an increasing collision rate and accelerating evaporation, indicating achievement of runaway evaporation; see Fig. 2.

An alternative evaporation path is developed to minimize the time to reach BEC. After a shorter magnetic field ramping process of 1 s, we ramp the field gradient from 38.9 G/cm at  $t=0$  to 41.3 G/cm in 0.5 s and then to 43.5 G/cm in another 1.5 s. Here we reach BEC in as short a period as 1.8 s of forced evaporation. Another 1 s evapo-

ration allows us to obtain  $4 \times 10^4$  atoms in an almost pure condensate, see Fig. 2(d). Despite the rapid increase of phase space density, the collision rate actually decreases by 25% at the end of evaporation. The truncation parameter and evaporation efficiency are  $\bar{\eta}=4.6$  and  $\bar{\gamma}_{ev}=1.9$ , respectively.

Throughout both evaporation processes, the peak density is moderate,  $n < 1.5 \times 10^{13} \text{ cm}^{-3}$ . The collision loss rate, dominated by three-body recombination [14], is below  $0.03 \text{ s}^{-1}$  at 20.8 G. Trap loss from collisions is negligible in the following discussion.

To understand the advantage of the trap-tilting scheme,

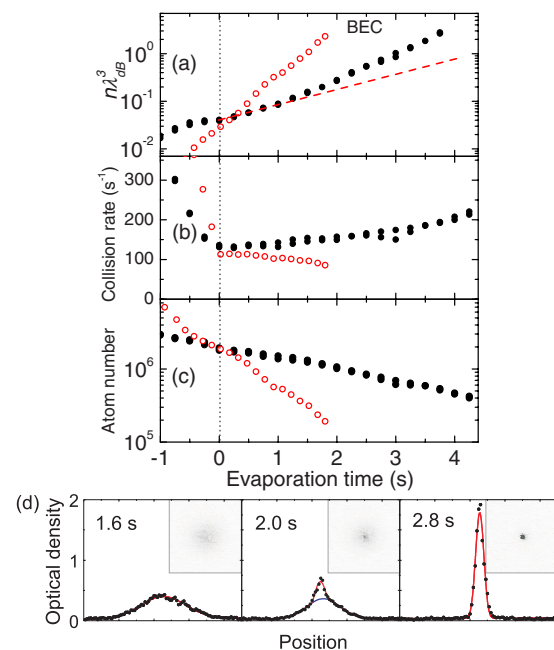


FIG. 2. (Color online) Performance of trap-tilting based forced evaporation: (a) Phase space density, (b) collision rate, (c) particle number, and (d) density profile. Two evaporation paths: 4 s (solid dots) and 1.8 s (open circles) are shown. The dashed line in (a) shows simple exponential increase. In (d), time-of-flight absorption images and single-line optical density profiles are taken from the 1.8 s evaporation path. The expansion time is 70 ms, and the field of view is  $1.2 \text{ mm} \times 1.2 \text{ mm}$ .

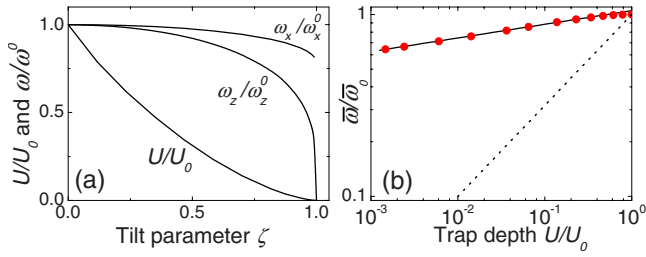


FIG. 3. (Color online) Depth and oscillation frequency of a tilted trap. (a) shows the calculated normalized trap depth and frequencies  $\omega_z$  and  $\omega_x = \omega_y$  as a function of the tilt  $\zeta$ , based on Eq. (1). In (b), mean trap frequencies are plotted against the trap depth for a tilted trap (solid dots) and for a weakened trap (dotted line). The solid line shows a power-law fit to the mean frequency, see Eq. (2).

we analyze evaporative cooling in a model potential. We combine the magnetic gradient potential and the gravitational potential as  $-\gamma mgz$ , where  $\gamma = B'/B_c' - 1$ . The total potential  $V(x, y, z)$  can be modeled as

$$V = -\frac{U_0}{2} (e^{-2(x^2+z^2)/w^2} + e^{-2(y^2+z^2)/w^2}) - \gamma mgz, \quad (1)$$

where the first two terms come from the two horizontal trapping beams, and the last term is the tilt potential. Here, we assume the two beams have the same beam waist  $w$  and peak light shift  $U_0/2$  for convenience.

We introduce the tilt parameter  $\zeta = e^{1/2} \gamma mgw / 2U_0$  to parameterize the trap depth  $U$  and trap frequencies  $\omega_{x,y,z}$ . Using Eq. (1), the trap depth and frequencies are evaluated as a function of  $\zeta$ , as shown in Fig. 3(a). All quantities are normalized to those of an untilted potential, where the trap depth is  $U_0$ , and the trap frequencies  $\omega_z^0 = \sqrt{2} \omega_x^0 = \sqrt{2} \omega_y^0 = \sqrt{4U_0/mw^2}$ . Note that the trap is unstable when  $\zeta \geq 1$ . In the range of  $10^{-3} < U/U_0 < 1$ , the geometric mean of the trap frequencies  $\bar{\omega} = (\omega_x \omega_y \omega_z)^{1/3}$  varies with the trap depth approximately as, see Fig. 3(b),

$$\frac{\bar{\omega}}{\bar{\omega}_0} \approx 1.05 \left( \frac{U}{U_0} \right)^{0.075(1)}, \quad (2)$$

where  $\bar{\omega}_0$  is the mean frequency of an untilted trap.

The key to fast, runaway evaporation in a tilted trap lies in the gentle, almost negligible weakening of the trap confinement when the trap depth decreases. As the trap depth decreases by a factor of 100, the trap frequency only decreases by 45% in the  $z$  direction and 14% in the other two directions, in contrast to the trap-weakening method, which reduces trap frequencies by a factor of 10 under the same condition. In general, a weakening trap with  $\bar{\omega} \propto U^\nu$  and  $\nu = 0.5$  shows a much stronger dependence on the trap depth than the tilting trap with  $\nu = 0.075$ .

The collision rate in a harmonic trap depends on the particle number, trap frequencies and temperature. Assuming  $\eta = U/k_B T > 6$  is a constant, we have

$$\Gamma \propto N \bar{\omega}^3 T^{-1} \propto U^{1/\alpha} U^{3\nu} U^{-1} \equiv U^\beta, \quad (3)$$

where  $\beta = 1/\alpha + 3\nu - 1$ ,  $\alpha > 0$  parametrizes the cooling efficiency by removing atoms [16]. Following the calculation in

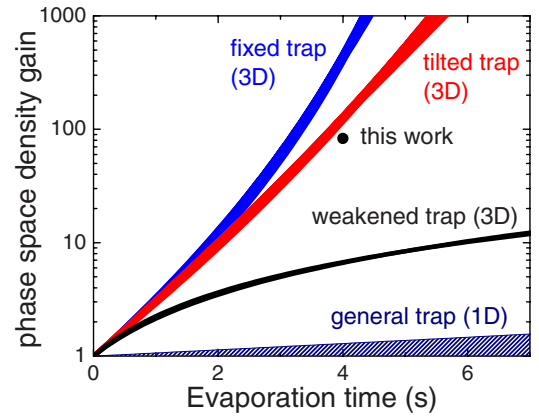


FIG. 4. (Color online) Evaporation speed: experiment (4 s path, solid dot) and models. We assume an initial collision rate of  $\Gamma_0 = 133 \text{ s}^{-1}$ ,  $\eta = \bar{\eta} = 6.2 - 6.8$  and no collision loss. The shaded area covers the 1D evaporation region with  $0 \leq \nu \leq 1$  and all possible  $\eta$ .

[17] with the trap frequency versus trap depth dependence,  $\bar{\omega} \propto U^\nu$ , we derive

$$\alpha = \frac{N dT}{T dN} = \frac{\eta + \kappa - 3}{3 - 3\nu}, \quad (4)$$

and  $\kappa > 0$  depends on the dimension of evaporation as discussed below.

The condition for runaway evaporation is given by  $\beta < 0$ . For the trap weakening scheme with  $\nu = 1/2$ ,  $\beta$  is positive for all  $\eta$ . Runaway evaporation is thus impossible. For the tilting scheme with  $\nu = 0.075$ , the exponent  $\beta$  is negative when  $\eta + \kappa > 6.58$ , suggesting runaway evaporation with increasing collision rate is possible.

Time evolution of the phase space density  $\phi(t)$  can be derived based on standard evaporation theory [16]. Assuming energetic atoms can leave the sample in all directions, we have  $\phi(t) = \phi(0)(1 + \lambda_{3D} \alpha \beta \Gamma_0 t)^{2/\beta - 1}$  and for  $\eta > 6$ ,  $\kappa_{3D} \approx (\eta - 5)/(\eta - 4)$  [17,18]. Here  $\Gamma_0$  is the initial collision rate and  $\lambda_{3D} \approx (\eta - 4)e^{-\eta}/\sqrt{2}$  [17,18] is the fraction of collisions producing an evaporated atom. Here we see that a negative  $\beta$  leads to a faster-than-exponential growth of the phase space density, which eventually diverges at time  $t = (-\lambda_{3D} \alpha \beta \Gamma_0)^{-1}$ . We compare the models and our experiment result in Fig. 4. To reach the same final phase space density, the trap-tilting scheme would require a much shorter evaporation time than the weakening scheme. For comparison, a potential with fixed trap frequency ( $\nu = 0$ ), e.g., radio-frequency based evaporation in magnetic traps, permits an even stronger runaway effect, see Fig. 4.

Remarkably, the performance of our evaporation is consistent with the three-dimensional (3D) evaporation model. The consistency of our evaporation speed with the 3D model is somewhat surprising. In a strongly tilted trap where hot atoms can only escape the trap in the tilted direction, it is generally expected that the evaporation will exhibit performance consistent with one-dimensional evaporation. Integration over the Boltzmann distribution on only this degree of freedom then results in a reduction of the evaporation rate by a factor of  $4\eta$  [19] and thus  $\lambda_{1D} = \lambda_{3D}/4\eta$ . Performance of

one-dimensional (1D) evaporation for all possible  $\eta$  is shown in the shaded area in Fig. 4. Our experiment result exhibits evaporation speeds much faster than the 1D prediction.

We suspect 3D-like evaporation in a tilted trap results from the inseparability of the potential and the existence of a saddle point located at the rim of the potential barrier, which can lead to stochastic single particle motion [19]. When atoms with sufficiently high energy are created by collisions, stochastic motion can allow them to efficiently find escape trajectories. If the energetic atoms have a high probability to escape, regardless of their initial direction of motion, evaporation is effectively three dimensional [19]. In realistic models, stochastization may also be induced by the intensity irregularities of the trapping laser beams.

To further investigate the “dimension of evaporation” in a tilted trap, we come back to  $\eta+\kappa$ , which parametrizes the energy removed by evaporating a single atom, or  $\eta+\kappa = -(k_B T)^{-1} dE/dN$ . For 3D evaporation, we expect  $\kappa_{3D} = (\eta - 5)/(\eta - 4)$ , which is  $\kappa_{3D} = 0.6(1)$  for our parameter  $\bar{\eta} = 6.5(3)$ ; for 1D evaporation, energy selectivity applies to the axial, but not the transverse motion, which has a mean energy of  $2k_B T$  per particle. Hence, we expect a higher energy removed per particle with  $\kappa_{1D} = \kappa_{3D} + 2 = 2.6(1)$  for our parameter [20]. Experimentally, we can test these predictions by evaluating  $\alpha$ , which has a simple dependence on  $\kappa$  as shown in Eq. (4). We show in Fig. 5 that our 4 s evaporation data is excellently fit to the power-law function with  $\bar{\alpha} = 1.46(2)$ . Using Eq. (4), we derive  $\kappa = 0.6(3)$ , which is consistent with the 3D value and confirms the 3D nature of the trap-tilt based evaporation.

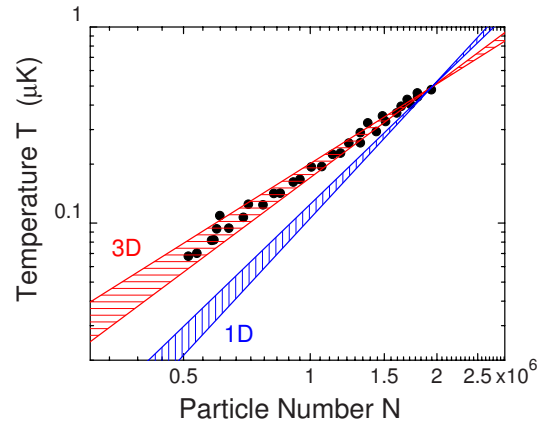


FIG. 5. (Color online) Temperature and particle number dependence. Based on the 4 s evaporation data (solid circles), the temperature shows a power-law dependence on particle number  $T \propto N^\alpha$ , with  $\alpha = 1.46(2)$ . For comparison, predictions from 3D and 1D evaporation models are shown using our experiment initial condition and  $\eta = 6.5 \pm 0.3$ .

This work is supported under ARO Grant No. W911NF0710576 with funds from the DARPA OLE Program, the NSF-MRSEC program under Grant No. DMR-0213745, and the Packard foundation. N.G. acknowledges support from the Grainger Foundation. We thank Jeffrey Gebhardt, Robert Berry, and Selim Jochim for the technical assistance in the early stage of the experiment.

- [1] J. Stenger, S. Inouye, D. M. Stamper-Kurn, H.-J. Miesner, A. P. Chikkatur, and W. Ketterle, *Nature (London)* **396**, 345 (1998).
- [2] S. Inouye, M. R. Andrews, J. Stenger, H.-J. Miesner, D. M. Stamper-Kurn, and W. Ketterle, *Nature (London)* **392**, 151 (1998).
- [3] S. Jochim, M. Bartenstein, A. Altmeyer, G. Hendl, S. Riedl, C. Chin, J. Hecker Denschlag, and R. Grimm, *Science* **302**, 2101 (2003).
- [4] M. Greiner, C. A. Regal, and D. S. Jin, *Nature (London)* **426**, 537 (2003).
- [5] M. D. Barrett, J. A. Sauer, and M. S. Chapman, *Phys. Rev. Lett.* **87**, 010404 (2001).
- [6] T. Weber, J. Herbig, M. Mark, H.-C. Nägerl, and R. Grimm, *Science* **299**, 232 (2003).
- [7] S. R. Granade, M. E. Gehm, K. M. O’Hara, and J. E. Thomas, *Phys. Rev. Lett.* **88**, 120405 (2002).
- [8] C. A. Regal, C. Ticknor, J. L. Bohn, and D. S. Jin, *Nature (London)* **424**, 47 (2003).
- [9] Y. Takasu, K. Maki, K. Komori, T. Takano, K. Honda, M. Kumakura, T. Yabuzaki, and Y. Takahashi, *Phys. Rev. Lett.* **91**, 040404 (2003).
- [10] The only possible runaway evaporation in a weakening trap is on resonant Fermi gas, see L. Luo, B. Clancy, J. Joseph, J. Kinast, A. Turlapov, and J. E. Thomas, *New J. Phys.* **8**, 213 (2006).
- [11] T. Kinoshita, T. R. Wenger, and D. S. Weiss, *Phys. Rev. A* **71**, 011602(R) (2005).
- [12] T. Kraemer, J. Herbig, M. Mark, T. Weber, C. Chin, H.-C. Nägerl, and R. Grimm, *Appl. Phys. B: Lasers Opt.* **79**, 1013 (2004).
- [13] A. J. Kerman, V. Vuletić, C. Chin, and S. Chu, *Phys. Rev. Lett.* **84**, 439 (2000).
- [14] T. Kraemer, M. Mark, P. Waldburger, J. G. Danzl, C. Chin, B. Engeser, A. D. Lange, K. Pilch, A. Jaakkola, H.-C. Nägerl, and R. Grimm, *Nature (London)* **440**, 315 (2006).
- [15] C. Chin, V. Vuletić, A. J. Kerman, S. Chu, E. Tiesinga, P. J. Leo, and C. J. Williams, *Phys. Rev. A* **70**, 032701 (2004).
- [16] W. Ketterle and N. J. Van Druten, *Adv. At., Mol., Opt. Phys.* **37**, 181 (1996).
- [17] K. M. O’Hara, M. E. Gehm, S. R. Granade, and J. E. Thomas, *Phys. Rev. A* **64**, 051403(R) (2001).
- [18] O. J. Luiten, M. W. Reynolds, and J. T. M. Walraven, *Phys. Rev. A* **53**, 381 (1996).
- [19] E. L. Surkov, J. T. M. Walraven, and G. V. Shlyapnikov, *Phys. Rev. A* **53**, 3403 (1996).
- [20] P. W. H. Pinkse, A. Mosk, M. Weidemüller, M. W. Reynolds, T. W. Hijmans, and J. T. M. Walraven, *Phys. Rev. A* **57**, 4747 (1998).